

Modification of the convective adjustment time-scale in the Kain–Fritsch eta scheme for the case of weakly forced deep convection over the Tibetan Plateau region

Chenghai Wang | Di Wu | Feimin Zhang

Key Laboratory of Arid Climate Change and Disaster Reduction of Gansu Province,
 College of Atmospheric Sciences, Lanzhou University, Lanzhou, China

Correspondence

Chenghai Wang, Key Laboratory of Arid Climate Change and Disaster Reduction of Gansu Province, College of Atmospheric Sciences, Lanzhou University, Lanzhou, China 730000.
 Email: wch@lzu.edu.cn

Present address: Di Wu, Department of Aviation Meteorology, College of Air Traffic Management, Civil Aviation University of China, Tianjin 300300, China.

Funding information

National Natural Science Foundation of China (NSFC), 91837205, 41805032, 41661144017, 91437217; China Special Fund for Meteorological Research in the Public Interest (Major projects), GYHY201506001-4.

Abstract

There is general uncertainty about the representation of clouds and convective precipitation in almost all models. Efforts to handle the convective parametrization scheme (CPS) in the grey zone ($\sim 1\text{--}5$ km horizontal grid spacing) are still imperative to the community, especially for the case of weakly forced deep convection. This study proposes a new convective adjustment time-scale (τ) for the Kain–Fritsch eta (KFeta) scheme in the Weather Research and Forecasting (WRF) model at high resolution, which differs from the current scale-aware function. The validation was made in three cases of weakly forced deep convection over the Tibetan Plateau. The results confirmed that modifying τ improves the simulation performance. In particular, the modified τ improved the simulated precipitation pattern, horizontal scale and intensity over the original scheme, which could be attributed to the enhanced rate at which convective instability generated by external factors (e.g. large-scale advection and surface turbulent fluxes) is removed by the parametrized convection. When τ is appropriately chosen, the CPS can be implemented in high-resolution simulations.

KEY WORDS

convective adjustment time, convective parametrization, mesoscale simulation, precipitation

1 | INTRODUCTION

Current regional weather prediction models are plagued by large uncertainty in terms of their treatment of clouds and precipitation (e.g. Maussion *et al.*, 2011; Wang and Yu, 2011; Zhang *et al.*, 2011; Su *et al.*, 2013; Bullock *et al.*, 2014; Dipankar *et al.*, 2015; Gao *et al.*, 2015). A better representation of the cloud and precipitation is necessary to reduce imprecision in current models' projections (Bony *et al.*, 2004; Stevens and Bony, 2013). The uncertainty in cloud simulation is mainly due to limitations of the parametrized shallow and

deep convective clouds (Dipankar *et al.*, 2015). In the past two decades, the prevailing treatment for representing deep convection in existing atmospheric models has experienced the transition from conventional cumulus parametrizations (Betts and Miller, 1986; Randall *et al.*, 1996; Ghan *et al.*, 2000) in general-circulation models to explicit simulation in cloud-resolving models (CRMs: Xu *et al.*, 1992; Xu and Arakawa, 1992; Grabowski *et al.*, 1996). However, in the intermediate scale range between them, separated by the grey zone or convection-permitting resolution, the mesoscale modelling community has long had difficulty in representing moist convective processes.

To reduce the uncertainty in cloud and precipitation simulation, many studies try to adopt models that are capable

Chenghai Wang and Di Wu contributed equally to this work and should be considered as joint first authors of this paper.

of resolving convection by fully explicit physics schemes without using a convective parametrization scheme (CPS) (e.g. Weisman *et al.*, 1997; Miura, 2007; Schlemmer *et al.*, 2011; Satoh *et al.*, 2014; Ban *et al.*, 2015). However, the hypothesis that high-resolution simulation (grid size: 1–4 km) can fully resolve convection has recently been questioned (e.g. Lean *et al.*, 2008; Gerard, 2015). Specifically, in some cases the subgrid organized vertical motions and convective condensation cannot be represented by the microphysics scheme alone (Kain and Fritsch, 1998; Deng and Stauffer, 2006). Thus, the CPS has always been a choice for subgrid-scale physics treatments. Using a CPS for convective clouds can also prevent the grid-point storms in mesoscale models (Zhang *et al.*, 1988).

In general, with the increases of model grid spacing, many CPSs are not adequately suitable for finer grid scales, especially for “grey zone” resolutions (\sim 1–5 km horizontal grid spacing) where neither a fully parametrized nor a fully explicit representation of deep convection can be used. Therefore, the assumptions of maintaining the quasi-equilibrium paradigm (proposed by Arakawa in 1969) for the current CPS can still apply by adding some auxiliary conditions at high horizontal resolution. One such key assumption involves the convective adjustment time-scale, which determines how rapidly convection acts to establish a neutral state (Betts, 1986). The study of Bretherton and Smolarkiewicz (1989) suggested that the convective adjustment time is related to the speed of the gravity waves and cloud grid spacing. Cohen and Craig (2004) provided convincing evidence on the basis of idealized CRM simulations that the convective adjustment time-scale is determined by the cloud grid spacing and environmental static stability. Their conclusion could not be suitable in the case where only a single convective cloud is present in a grid cell as is generally true at high resolution (grey zone). Kain and Fritsch (1990), and Betts (1997) assumed that the convective adjustment process proceeds systematically as convective updraught–downdraught couplets move over an area, ingesting low-level unstable air and leaving more stable air in their wake. Accordingly, it seems to be reasonable to consider the grid spacing of a model as a parameter called the convective adjustment time-scale. However, at small grid spacing or high wind speed, the equation developed by Kain and Fritsch (1993) for calculating the convective adjustment time-scale may approach its limit (Stensrud, 2007). To handle the transition between explicit physics and implicit cloud parametrization schemes, Zheng *et al.* (2016) introduced a scale-aware approach by calculating so-called “function for convective adjustment time-scale” into the Weather Research and Forecasting (WRF) model v3.7 (Skamarock *et al.*, 2008). Specifically, the convective adjustment time-scale is calculated by multiplying a scaling parameter associated with the horizontal grid spacing. However, the effects of this function on the simulation of convective precipitation in the Tibetan

Plateau region are still not clear to the community. In other words, whether all convection processes can be improved with the “scale awareness” is still an open question.

The parametrization of convective adjustment time should be transformed from the formulation of horizontal grid spacing to one that represents the time-scales of convective cloud vertical overturning. Bullock *et al.* (2015) proposed a formulation for convective adjustment time-scale based on the depth of the buoyant layer and the convective velocity scale. Since the model vertical resolution and height is sufficient to resolve the depth of convection, it could be applied to almost all convective cloud types. In addition, with the increase of the horizontal grid resolution, the parametrized cloud radius in the original Kain–Fritsch eta (KFeta) CPS scheme could not be suitable to consider for more small-scale clouds. The work of Narita (2010) suggested that the KFeta CPS got better results by changing the cloud radius to a smaller value. Thus, a simple modification for the cloud radius is given when conducting the high-resolution simulation.

Owing to its unique and complex terrain, the Tibetan Plateau (TP) is an ideal test case for validating model performance. The TP also prominently affects the global climate system (Xu *et al.*, 2008; Dong *et al.*, 2016), and the many unique characteristics of weather events over the TP have proven challenging to simulate (Boos and Kuang, 2010; Huang *et al.*, 2010; Xu *et al.*, 2012; Wang *et al.*, 2014; Yan *et al.*, 2016). In summer, many convective events are frequently initiated by strongly enhanced surface diabatic heating and dynamic lifting by topographic forcing (Fu *et al.*, 2006a; Li and Zhang, 2016; Wang and Wang, 2016). Meanwhile, since the water vapour amounts over the TP are relatively low in summer, the convective available potential energy (CAPE) is lower than in most other continental regions during this season (Fu and Liu, 2007). These characteristics contribute to convective clouds with short lifetimes (Chen *et al.*, 2017). Luo *et al.* (2011) compared the deep convection over South Asia and subtropical North America over the summer seasons from 2006 to 2009 with the data sourced from CloudSat and Cloud–Aerosol Lidar and Infrared Pathfinder Satellite Observations (CALIPSO). They concluded that the deep convection typically has a smaller horizontal scale and smaller CAPE values over the TP than elsewhere, which is consistent with the studies of Houze *et al.* (2007) and Romatschke *et al.* (2010). Meanwhile, the deep convection is weaker and less well organized in the TP region than that in the surrounding regions because of its higher mean surface elevation (about 4 km). It can be concluded that the deep convective systems are generally weaker (associated with smaller CAPE: Luo *et al.*, 2011) over the TP than elsewhere, leading to reduced amounts of precipitation. These features, which distinctly differ from most other continental regions, are not explicitly considered in existing model schemes.

This study aims to answer the question: can CPS in the grey zone be improved to better simulate precipitation by modifying the duration of convective processes in the Kain–Fritsch eta (KFeta) scheme? To overcome the challenge of the grey zone, in which deep convection is only partly resolved in the horizontal direction, we propose a new convective adjustment time-scale based on the vertically resolvable deep convective clouds. Through three cases of convective precipitation simulations in the TP, where deep convection is generally weakly forced, both the scale-aware KFeta scheme and the new scheme are validated against the observations.

The remainder of this article is organized as follows: section 2 describes the WRF model and the experimental designs, and section 3 simulates the convective precipitation event and compares the results with observations. Section 4 introduces a new method of computing the convective adjustment time-scale in the KFeta scheme. The performance of the modified convective adjustment time-scale is evaluated in section 5. A summary and conclusions are presented in section 6.

2 | MODEL AND EXPERIMENTAL DESCRIPTIONS

2.1 | Model configuration

The convective precipitation events are simulated in the non-hydrostatic mesoscale model WRF v3.7.1. The configuration includes one-way nesting with horizontal grid spacings of 27, 9 and 3 km (denoted as D01, D02 and D03, respectively) and 40 vertical levels (with the top level at 50 hPa). The outermost domain D01 covers most of the Asian continental area with 185×205 grid points, the intermediate domain D02 covers the entire TP area with 229×379 grid points, and the innermost domain D03 covers the middle and eastern TP with 313×382 grid points (Figure 1). Based on previous studies on the simulation of precipitation over the TP (e.g. Huang *et al.*, 2010; Wang *et al.*, 2014), the physical schemes include the WRF Double Moment six-class microphysics scheme (WDM6: Lim and Hong, 2010), the Dudhia short-wave radiation scheme (Dudhia, 1989), the Rapid Radiative Transfer Model (RRTM) long-wave radiation scheme (Mlawer *et al.*, 1997), the Yonsei University (YSU) planetary boundary-layer scheme (Hong *et al.*, 2006), the Revised MM5 Monin–Obukhov surface layer scheme (Jimenez *et al.*, 2012), and the Unified Noah land-surface model land surface scheme (Tewari *et al.*, 2004). The interactions between the subgrid cloud fraction and radiation (*cu_rad_feedback*) included in the KFeta cumulus scheme (Kain, 2004) is activated in the D01 and D02 domains.

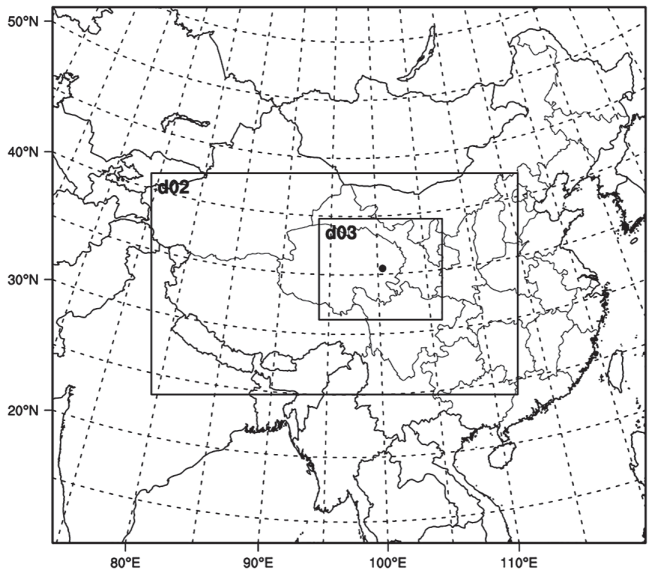


FIGURE 1 Domain of the Weather Research and Forecasting (WRF) simulations described in Table 1. The dot indicates the centre of the domain

The initial conditions and boundary conditions (ICBC) are sourced from the National Centers for Environmental Prediction (NCEP) final reanalysis data (FNL) (Kalnay *et al.*, 1996), which are resolved to 1° and 6 h. The simulation of the convective precipitation event of Case 1 (described below) is initialized at 0200 LST 1 July (1800 UTC 30 June) 2010, integrated for 36 h. Another two convective precipitation cases, which occurred on 10–11 August 2010 (Case 2) and 17–18 August 2011 (Case 3), are also considered. The outputs are every 3 h in D01, and every 1 h in D02 and D03. The time step for the outermost domain is 120 s. The major analyses are performed on the D03 model outputs.

2.2 | Experimental design

In the original experiment (OEXP), the default KFeta scheme was applied in WRF v3.7.1. To understand the effects of CPS in a high-resolution simulation (grid spacing $\sim 1\text{--}10$ km), we performed the OEXP-CU experiment, which turns on the convective parametrization scheme, and the interaction between the subgrid cloud and radiation is also considered in the D03 domain, otherwise it is identical to OEXP. To compare the performances of OEXP, OEXP-CU and the scale-awareness scheme in a high-resolution simulation of convection precipitation, we also ran the MEXP experiment, which is configured identically to OEXP but adopts the Multi-Scale KF (MSKF: Zheng *et al.*, 2016) CPS in all domains. MEXP includes a scale-awareness function and was successfully introduced in WRF v3.7. Three cases of convective precipitation events over the TP were simulated. The above experimental designs and numerical simulations are described in Table 1.

TABLE 1 Descriptions of the simulation experiments conducted in this study

| Case number | Simulation name | Description |
|-------------|-----------------|--|
| 1 | OEXP | Original KFeta scheme only in D01, D02 |
| | OEXP-CU | As in OEXP, but with the CPS turned on in D03 |
| 2 | MEXP | MSKF scheme run in all domains |
| | MEXP1 | Modified threshold of τ in all domains and cloud radius in D03 |
| 3 | MEXP2 | Modified both the threshold and formulation of τ in all domains and cloud radius in D03 |
| | OEXP | Original KFeta scheme only in D01, D02 |
| 2 | MEXP | MSKF scheme run in all domains |
| | MEXP2 | Modified both the threshold and formulation of τ in all domains and cloud radius in D03 |
| 3 | OEXP | Original KFeta scheme only in D01, D02 |
| | MEXP | MSKF scheme run in all domains |
| | MEXP2 | Modified both the threshold and formulation of τ in all domains and cloud radius in D03 |

3 | PERFORMANCES OF SIMULATIONS OF CONVECTIVE PRECIPITATION OVER THE TP

3.1 | Observed convective precipitation event

The study mainly focuses on Case 1, and the data of this event are obtained by infrared satellite, reanalysis datasets, and meteorological observations. Figure 2a,b show the brightness temperatures from the Chinese Feng-Yun-2E (FY2E) infrared satellite. During the afternoon of 1 July 2010 (1400 LST or 0600 UTC; local time is UTC + 8 h), several convective clouds drifted over the northeastern TP (Figure 2a). Over the following 6 h, the scattered cloud evolved into a coherent convective cloud system that produced precipitation and moved northeastward (near 34°N, 100°E) across the northeastern TP at 2000 LST (1200 UTC, Figure 2b). Meanwhile, the 6-hourly 1° NCEP FNL reanalysis data (Kalnay *et al.*, 1996) revealed a 500 hPa trough within this region, and the convective cloud system was driven predominantly by a strong 200 hPa southwesterly flow (Figure 2c). The atmosphere was weakly unstable; for instance, the CAPE of the Yushu sonde observation (33.01°N, 97.01°E; Figure 2d) was only 42.61 J/kg at 1200 UTC 1 July 2010. According to the observed rainfall from the Automatic station and the Climate Prediction Center's morphing technique (CMORPH) hourly precipitation fusion products (resolved to 0.1°) of the China Meteorological Data Service Center, the rainfall was approximately 35 mm with a relatively small areal coverage, that is, the 7 h accumulated precipitation was not too high (Figure 2d). Around 0200 LST on 2 July (1800 UTC 1 July), the convective system had propagated to the border of the northeastern TP and weakened,

and the precipitation also began to decrease. Obviously, this deep convective system occurred over a relatively small area, under weak CAPE conditions, consistent with typical deep convective features over the TP.

3.2 | Biases in the original convective parametrized simulation

The convective precipitation simulated by OEXP and OEXP-CU from D03 outputs (interpolated to the same resolution of observations; Figure 3d–i) were compared with the CMORPH hourly precipitation fusion products of the China Meteorological Data Service Center (approximately 8 km grid spacing; Figure 3a–c). Both the OEXP and OEXP-CU simulations failed to capture the observed rainfall structures and underestimated the rainfall in the northern portion of the study area, while producing too much rain in the far southern portion. The simulated convective systems, in both cases, propagate from west to east and are somewhat faster than observed (Figure 3d–i), which indicates that there are defects in the area of simulated precipitation in the OEXP and OEXP-CU experiments.

3.3 | Performance of scale-aware scheme in convective precipitation

Figure 4a–c show the precipitation simulated by MEXP on the D03 outputs. Compared with the OEXP and OEXP-CU simulations, the scale-aware scheme does not generate an improvement for the precipitation simulation performance. Similarly, the location of precipitation is southeast of the observed rainfall areas, and the total amount of precipitation is again underestimated.

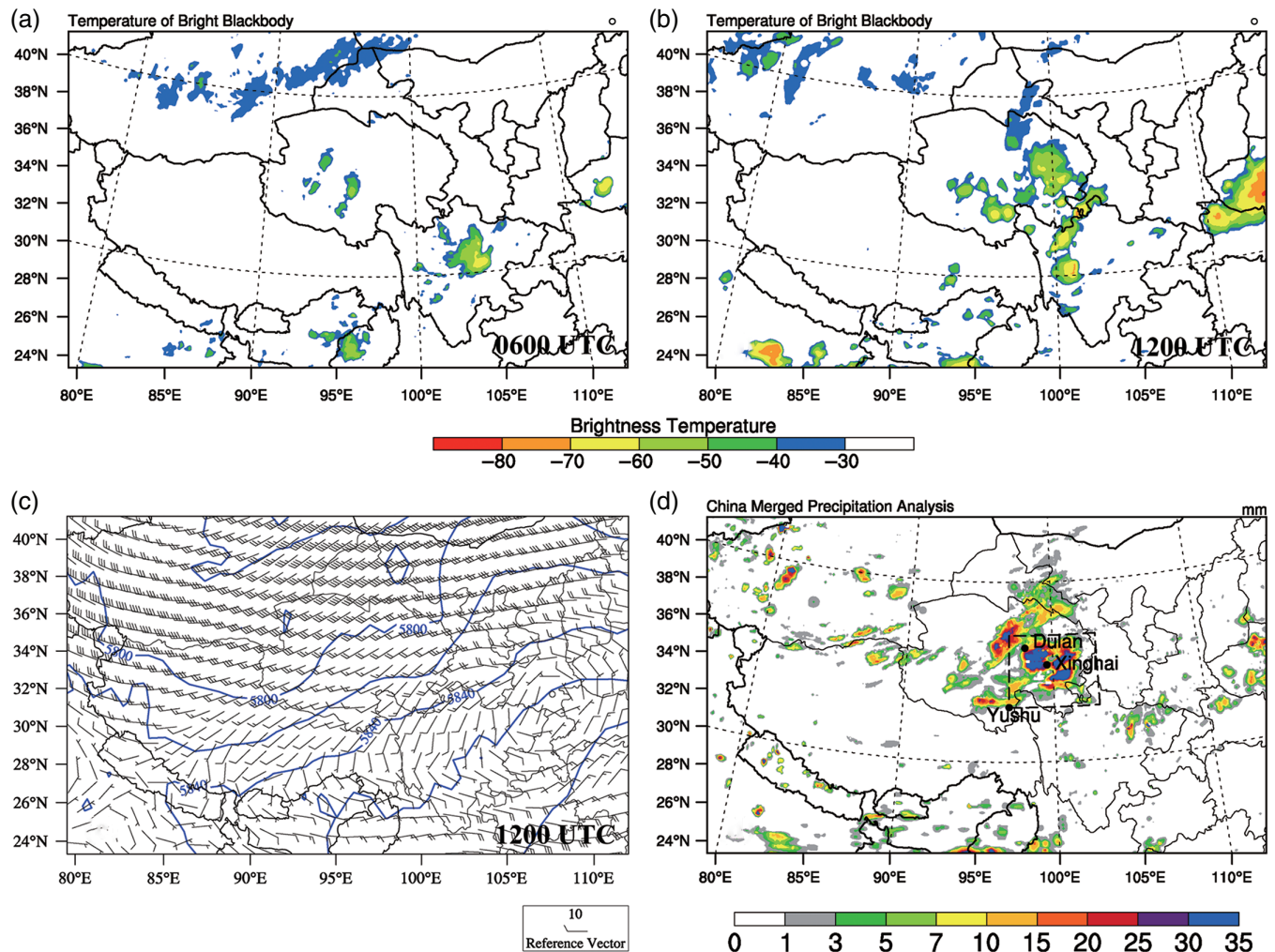


FIGURE 2 Meteorological conditions of the convective process over the TP. (a) 0600 UTC and (b) 1200 UTC 1 July brightness temperatures (shaded; °C), taken from the hourly temperature blackbody equivalent of the Chinese Feng-Yun-2E (FY2E) infrared (IR) satellite; (c) 1200 UTC 1 July, 500 hPa geopotential heights (blue solid lines; gpm) and 200 hPa wind (vectors; m/s) fields, taken from the 6-hourly 1° National Centers for Environmental Prediction (NCEP) Final (FNL) reanalysis data; and (d) observed 7 h accumulated precipitation (shaded; mm) during 0900–1600 UTC on 1 July 2010, taken from the automatic station and the CMORPH hourly precipitation fusion products (resolution = 0.1°) of the China Meteorological Data Service Center. The black dots in (d) pinpoint the Yushu (33.01°N, 97.01°E), Dulan (36.30°N, 98.10°E) and Xinghai (35.35°N, 99.59°E) observation stations

4 | MODIFICATION OF CONVECTIVE ADJUSTMENT TIME-SCALE

Though the effects of CPS become less significant with increasing model resolution, there is still a need to parametrize the effects of clouds that still are not resolved by explicit physics schemes (Zheng *et al.*, 2016). Thus, the cumulus convection parametrization scheme is an important component of grey-zone WRF simulations of clouds and precipitation (Zhang *et al.*, 1988; Kuo *et al.*, 1997; Mahoney, 2016). Developed by Kain (2004), the KFeta scheme is based on the original Kain–Fritsch (KF) scheme (Kain and Fritsch, 1990; 1993), which models a bulk cloud plume with the exchange of mass flux between clouds and the environment. This scheme has been popularly adopted in weather and

climate studies (e.g. Kain and Fritsch, 1998; Cohen, 2002; Alapaty *et al.*, 2012), so was also adopted in the present study. In the KFeta scheme, τ is an important factor that determines the rate at which convective instability is removed by the subgrid-scale convection; that is, the response time of the subgrid convective process to the large-scale environment. The convective adjustment process can be roughly assumed as instantaneous (Manabe *et al.*, 1965), and then is considered to be temporally constant directly equivalent to the model time step or a few time steps (Betts, 1986). Although this factor is sensitive and has been tested through trial and error (e.g. Emanuel *et al.*, 1994; Mishra and Srinivasan, 2010), it lacks a universally accepted value or formulation. Moreover, shortcomings of the KFeta scheme may emerge at fine resolutions (Stensrud, 2007). Bullock *et al.* (2015) also

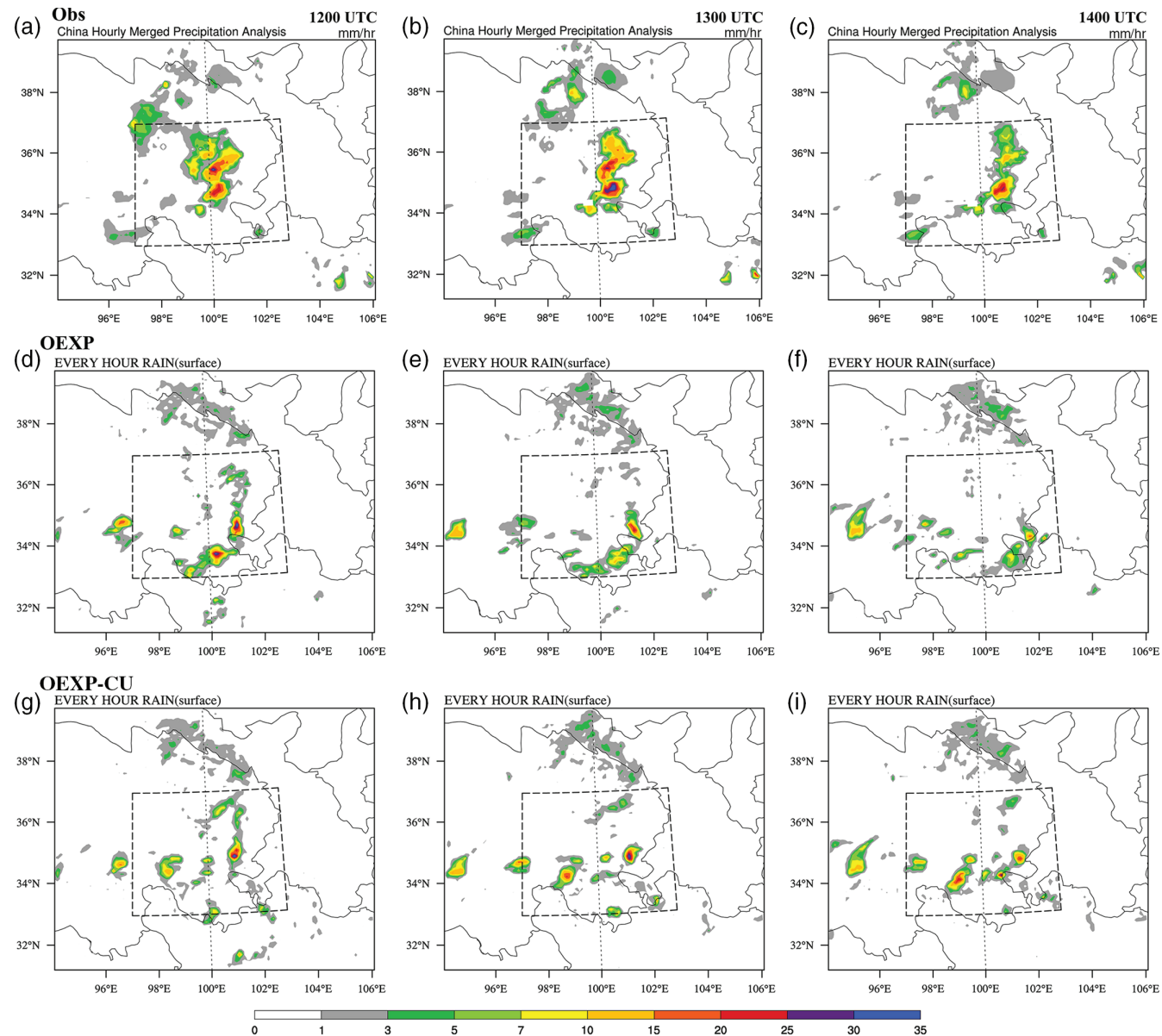


FIGURE 3 The 1 h accumulated precipitation at the surface (mm/h) beginning at 1200 UTC (left), 1300 UTC (middle) and 1400 UTC (right) on 1 July 2010. Data were taken from (a–c) the observed precipitation at the automatic station and CMORPH hourly precipitation fusion products (resolution = 0.1°) of the China Meteorological Data Service Center, the simulated D03 outputs of (d–f) OEXP and (g–i) OEXP-CU. The dashed box encloses the main rainfall area

proposed a dynamically based formulation of τ in the KFeta scheme with a 12 km grid spacing.

Whether the CPS should be employed in the grey zone of horizontal grid spacing (i.e. <10 km) continues to be debated. Zheng *et al.* (2016) suggested that changing the grid resolution will change the convective adjustment time. Accordingly, we investigated how τ influences convective precipitation over the TP in the KFeta scheme. Specifically, we modified τ to make it independent of grid resolution, then applied it in a high-resolution simulation.

Based on early observations of typical cloud lifetimes and experimental tests, Kain and Fritsch (1993) suggested that the τ threshold ranges from 1,800 to 3,600 s in the KFeta

scheme. In general circulation models, the τ threshold ranges from approximately one to a few hours (Collins *et al.*, 2006). Bechtold *et al.* (2008) expressed τ as a function of cloud depth and reported a range of 600 s to 3 h in global models.

One alternative way of making the KF scheme scale-aware is to specify τ so that the effects of the scheme gradually become negligible as the horizontal grid spacing is made finer. Done *et al.* (2006) suggested that an upper limit of 3,600 s satisfies the quasi-equilibrium condition originally proposed by Arakawa (1969) (see also Arakawa and Schubert, 1974). To maintain some form of quasi-equilibrium at high resolution, the local convective adjustment should respond

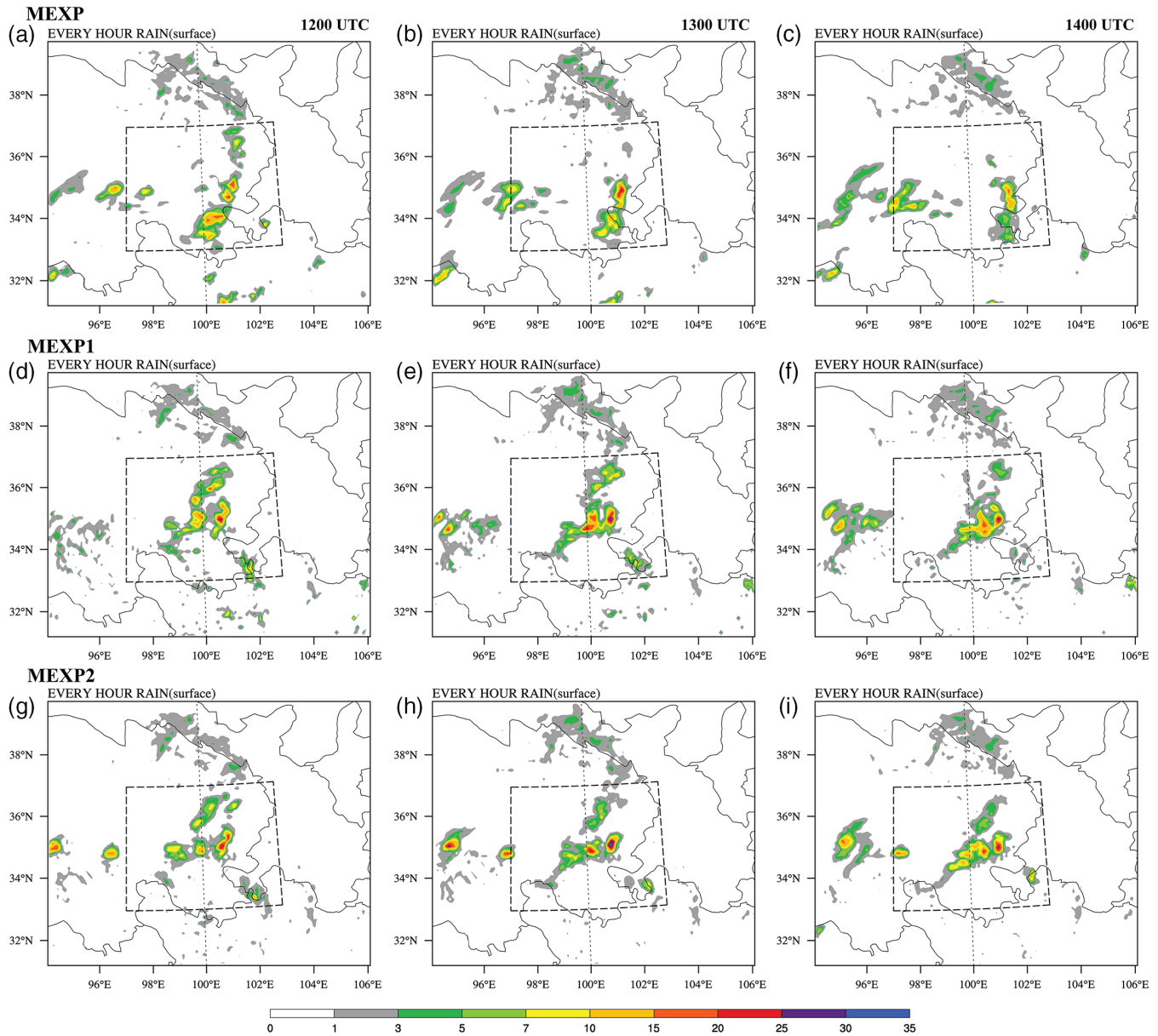


FIGURE 4 Same as Figure 3, but for the simulated precipitation from (a–c) MEXP, (d–f) MEXP1 and (g–i) MEXP2 experiments

much more rapidly than the large-scale forcing. As suggested by Bechtold *et al.* (2008), we thus adopted a lower limit of 600 s rather than the original 1,800 s. This modification allows rapid response of the convection development, subsequently shortening the convection lifetime for high-resolution simulations.

In the KFeta scheme, the convective adjustment time scale $\tau(s)$ was originally formulated as

$$\tau = \frac{dx}{|\bar{v}_{\text{avg}}|}, \quad (1)$$

where dx is the grid spacing and v_{avg} is the average horizontal wind speed in the lifting condensation level (LCL) and the middle troposphere. Equation 1 describes that the convective cloud system moves horizontally across the individual grid

spacing under dominant advection processes, and τ depends on the horizontal grid distance. However, due to either the smaller horizontal grid spacing or the sudden increase in averaged horizontal wind speeds, their equations could break down. Moreover, it is not physically justified based on the convective adjustment process in terms of either gravity wave propagation or the convective overturning time-scale. Thus, the original Equation 1 is not recommended on grey-zone scales. Additionally, the horizontal airflow over the TP is rendered heterogeneous by the complex terrain; the obviously undulating mountains contain wetlands, lakes, rivers, grasslands, meadows, and other features. The horizontal scale of convective clouds is smaller, and the convection more localized, than in most regions. Thus, by focusing on the vertical convection process and the time-scale of convective

vertical overturning, a revised formulation for the convective adjustment time-scale analogous to but different form that of Bullock *et al.* (2015) is given as follows

$$\tau = \frac{Z_{\text{Top}} - Z_{\text{LCL}}}{W_c}, \quad (2)$$

where Z_{Top} and Z_{LCL} are the top and bottom heights of the cloud, respectively, and W_c is the vertical velocity. In Bullock *et al.* (2015), the convective velocity w_c was diagnosed using the convective cloud-mass flux and the cloud work function. However, based on natural convective motions over a range of scales, from microscale turbulence to organized convective circulations (analysed by Done *et al.*, 2006), the vertical velocity W_c here includes both the local-scale and large-scale effects

$$W_c = W_{\text{LCL}} + W_{\text{LS}}, \quad (3)$$

where W_{LCL} is the vertical velocity of the rising parcel at the LCL, and W_{LS} is the imposed large-scale vertical velocity proposed by Zhang and McFarlane (1995), which is based on the concept that deep convection in the atmosphere is enhanced in regions of large-scale ascent and suppressed in regions of subsidence, with the motivation to improve the performance of simulation for convective response. W_{LS} is formulated as

$$W_{\text{LS}} = 4W_{\text{mid}}(P_B - P_{\text{LCL}})(P_{\text{LCL}} - P_T)/(P_B - P_T)^2, \quad (4)$$

where W_{mid} is the grid-resolved vertical velocity in the middle troposphere, P_{LCL} is the pressure of the LCL, and P_B and P_T are the bottom and top pressures in the model, respectively. Similarly, the τ threshold is restricted to the range 600–3,600 s. In addition, for the D03 domain, the cloud radius threshold of the original KFeta scheme is also modified. The original parametrized cloud radius R is defined as

$$R \begin{cases} 1000, & W_{\text{KL}} < 0 \\ 2000, & W_{\text{KL}} > 10, \\ 1000(1 + W_{\text{KL}}/10), & 0 \leq W_{\text{KL}} \leq 10 \end{cases} \quad (5)$$

where R (m) is the cloud radius, $W_{\text{KL}} = w_g - c(z)$, and w_g is grid-resolved vertical velocity at the LCL (cm/s), $c(z)$ is the threshold vertical velocity described by Kain (2004). The newly parametrized cloud radius equation can be given as

$$R \begin{cases} 500, & W_{\text{KL}} < 0 \\ 1000, & W_{\text{KL}} > 10, \\ 500(1 + W_{\text{KL}}/10), & 0 \leq W_{\text{KL}} \leq 10 \end{cases} \quad (6)$$

Moving from Equation 5 to Equation 6 changes the typical value of cloud radius to keep the KFeta scheme suitable for high resolution, which allows more small-scale clouds within a grid cell to be parametrized.

Equations 2–4 and 6 establish the modified scheme in this study, which is defined as the BW (Bullock–Wang) scheme expressed conveniently for the present study. The BW scheme includes the modification for the threshold and formulation of τ and the convective cloud's radius and establishes the relations between τ and the vertical velocity and depth of a convective system; were the depth of the convective system to increase, the convective adjustment times would be longer. Note that the dependence on horizontal grid spacing (scale-aware function) has been removed. In this scheme, τ represents the convective turnover time at resolved scales in high-resolution simulations (Bullock *et al.*, 2015).

To validate the newly proposed approach, the effects of the modified τ were evaluated in two additional experiments (Table 1). In the first experiment (designated MEXP1), the convective parametrization scheme was activated in all domains, with the modified τ threshold adopted. The second experiment (designated MEXP2) is the same as MEXP1, but adopting the modified τ threshold, the new scheme for τ , and the modified cloud radius at the same time. By comparing the simulation performances of MEXP, MEXP1 and MEXP2, we can determine whether the high-resolution simulation depends on the scale-aware function, at least in the TP region.

5 | VALIDATION OF THE NEW SCHEME ON CONVECTIVE PRECIPITATION

5.1 | Effect of the scheme on precipitation simulation

Figure 4 shows the simulated convective precipitation of Case 1 from the D03 outputs in MEXP, MEXP1 and MEXP2. Compared with the hourly precipitation results of OEXP, OEXP-CU and MEXP, both MEXP1 and MEXP2 generated a northeast–southwest oriented, east–west propagating precipitation band that resembles the observed precipitation band, although the rainfall intensity was still slightly underestimated, and the precipitation system lagged the observed system (Figure 4d–i). The simulated precipitation emerged at approximately 1400 LST (0600 UTC) on the northeastern TP. At 1800 LST (1000 UTC), the convective cloud system had matured, and precipitation occurred near Dulan Station (36.30°N, 98.10°E; Figure 2d). At 2000 LST (1200 UTC), the precipitation system moved eastward across Xinghai Station (35.35°N, 99.59°E), and the rainfall began to intensify (Figure 4d,g). At 2200 LST (1400 UTC), the system continued propagating as the convective system approached the border of the northeastern TP (Figure 4f,i), and the rainfall had attained its peak. Thereafter, the precipitation began to weaken, and the convective cloud gradually dissipated. The

simulated precipitation ended 2 h later than the observed precipitation. However, the simulations in OEXP, OEXP-CU and MEXP only present a few areas of precipitation that were almost on the southeast side of the TP region (Figures 3d–i and 4a–c). These results highlight the stronger performance of MEXP2 than of MSKF (MEXP), especially when simulating the precipitation location. Therefore, the new approach is reasonable. In the MSKF scheme of MEXP, τ depends on the horizontal grid distance. The present results demonstrate that the BW scheme, in which τ is not scale-aware, outperforms the MSKF scheme in the TP region. Comparing MEXP and MEXP2, it is clear to see that MEXP2 outperforms MEXP.

To further confirm the performance of the BW scheme in the process of convective precipitation, Figure 5 shows the simulation of precipitation of Case 2. Results indicate that the precipitation location from OEXP and MEXP experiments exhibit an obvious northward shift compared with observation at 2300 LST (1500 UTC; Figure 5d,g) and miss the subsequent precipitation process after 0100 LST (1700 UTC; Figure 5e,f,h,i). However, the simulation from MEXP2 well captures this process (Figure 5j–l), especially at 0100 LST (1700 UTC; Figure 5k), and the rainfall amount is closer to the observation. It should be noted that the WRF model has always had difficulty in reproducing the mesoscale precipitation process accurately over the TP region (Maussion *et al.*, 2011). The BW scheme provides some improvements over the KF and Multi-scale KF scheme, though there are still some biases in the precipitation location.

Similar results are also found in Case 3 (Figure 6). The OEXP and MEXP experiments not only wrongly simulated the precipitation centre position, but also under-predicted the amount of precipitation, while overestimating its downstream area (Figure 6d–i). However, these results are ably remedied by the MEXP2 experiment. The above results further illustrate that convective precipitation can also be well reproduced by the modified convective adjustment time-scale, which can be considered as a compliment for scale-awareness.

Table 2 provides the quantitative evaluations of the simulated precipitation for the three cases. Listed are the bias scores and pattern correlations between the observed precipitation and the precipitation simulated by each experiment. As confirmed in the hourly bias scores, MEXP2 with the BW scheme outperformed the other methods in general. Meanwhile, the pattern correlation coefficient demonstrates an improved precipitation pattern with MEXP2. The Equitable threat scores (ETSSs; Wilks, 1995) are also calculated for the three cases for the 24 and 12 h accumulated precipitation, against the CMORPH hourly precipitation fusion products. Results in Figure 7 clearly show that all experiments with the BW scheme (MEXP2) lead to a better ETS, compared with OEXP and MEXP. Compared with the performance of

hourly precipitation distribution, the statistical results of accumulated precipitation seem to be more obvious. These results indicate that modifying τ improves the performance of the convective precipitation simulation over the TP region, especially in the BW scheme on high-resolution domains. They also verify that the simulated precipitation is sensitive to the formulation of τ . Therefore, the BW scheme does not require a scale-aware function in the TP region.

5.2 | Effect of the scheme on the mechanism of the convective process

To illustrate the cloud dynamics in the modified scheme, Figure 8 gives the relations between the time-averaged CAPE (panels a–c), time-averaged cloud depth (panels d–f) and time-averaged maximum updraught mass flux (UMF) (panels g–i) of each grid column in different experiments with the τ over the entire period for Case 1. These results are derived from the D03 outputs of each experiment. In the convective precipitation process of OEXP-CU, the convective adjustment time is long ($\tau < 1,200$ s) but the CAPE is relatively weak (CAPE < 700 J/kg) (Figure 8a). Adjusting the lower limit of τ (MEXP1) introduces scattering in the region (CAPE < 900 J/kg and $\tau < 800$ s), demonstrating a shorter convective adjustment time and a stronger convective instability than in OEXP-CU (Figure 8b). Furthermore, the improved scheme (MEXP2) gives CAPE < 900 J/kg and $\tau < 600$ s, and the CAPE and τ are strongly related (Figure 8c). Moreover, during weak convection (small CAPE values), the scatters at long convective adjustment times in Figure 8a,b are replaced by shorter convective adjustment times in Figure 8c. The MEXP2 results confirm the applicability of the BW scheme to deep convective clouds with shallow depth over the TP region. Also, the convective adjustment time-scales are shorter in MEXP2 than in OEXP-CU and MEXP1 (Figure 8d–f). These results highlight that rapid τ may be suitable for the weak and deep convective clouds over the TP area. More importantly, shortening the τ will influence the convectively generated changes, such as temperature and hydrometeor feedback to the microphysical scheme.

To better relate the experimental differences to precipitation, the convection was expressed in terms of the dimensionless UMF (Kain *et al.*, 2003). The dimensionless UMF also determines the intensity and distribution of the convective precipitation as the instability settles into a quasi-equilibrium state. In the scatterplot of OEXP-CU, the maximum UMF is a slowly increasing function of τ (Figure 8g), reflecting the upward transportation of the cloud base mass flux. This implies that the convective adjustment time can affect the energy and the mass exchange in the convective cloud, producing unrealistic stability and convective balance. However, when the lower limit of τ is changed in MEXP1 (Figure 8h), the maximum UMF increases at $\tau < 300$ and $\tau > 600$ s, which

TABLE 2 Pattern correlation coefficients of 12 h accumulated precipitation and hourly bias scores between observation and simulations

The bias score is the ratio of the simulated area-averaged precipitation to the observed result. A bias score of 1.00 denotes perfect performance. The farther the score deviates from 1.00, the worse the simulation is.

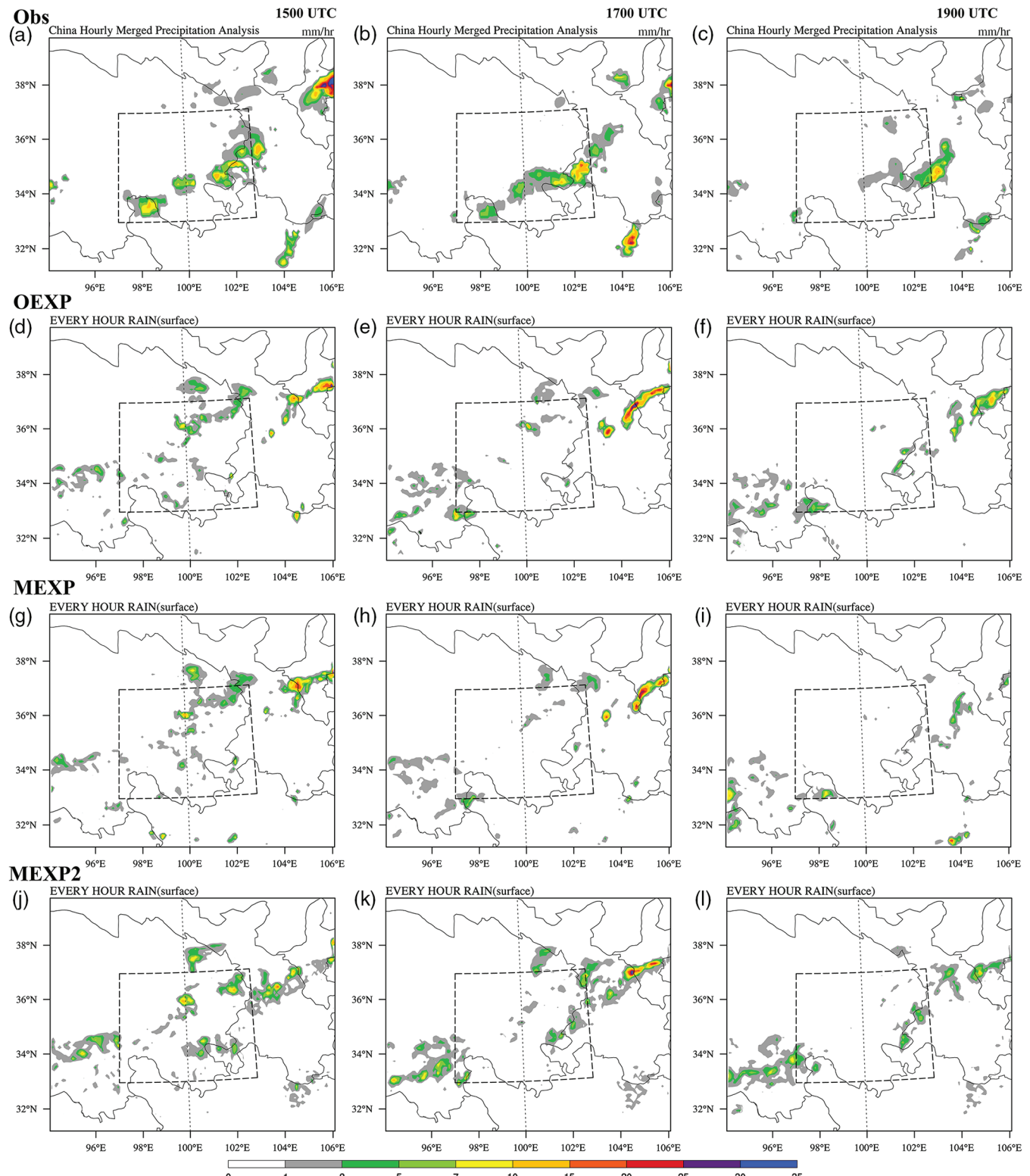


FIGURE 5 Same as Figure 4, but for Case 2 at 1500 UTC (left), 1700 UTC (middle) and 1900 UTC (right) on 10 August 2010 from (a–c) the observations, simulated D03 outputs of (d–f) OEXP, (g–i) MEXP and (j–l) MEXP2

is inconsistent with the observations (Done *et al.*, 2006). Meanwhile, MEXP2 yields a stronger positive correlation between UMF and τ than OEXP-CU (Figure 8i). These characteristics simulated by the modified scheme demonstrate

realistic behaviour and are consistent with the observed characteristics (Kain *et al.*, 2003).

Figure 9 plots the time series of τ at the Dulan and Xinghai observational stations, calculated from the D03 outputs in

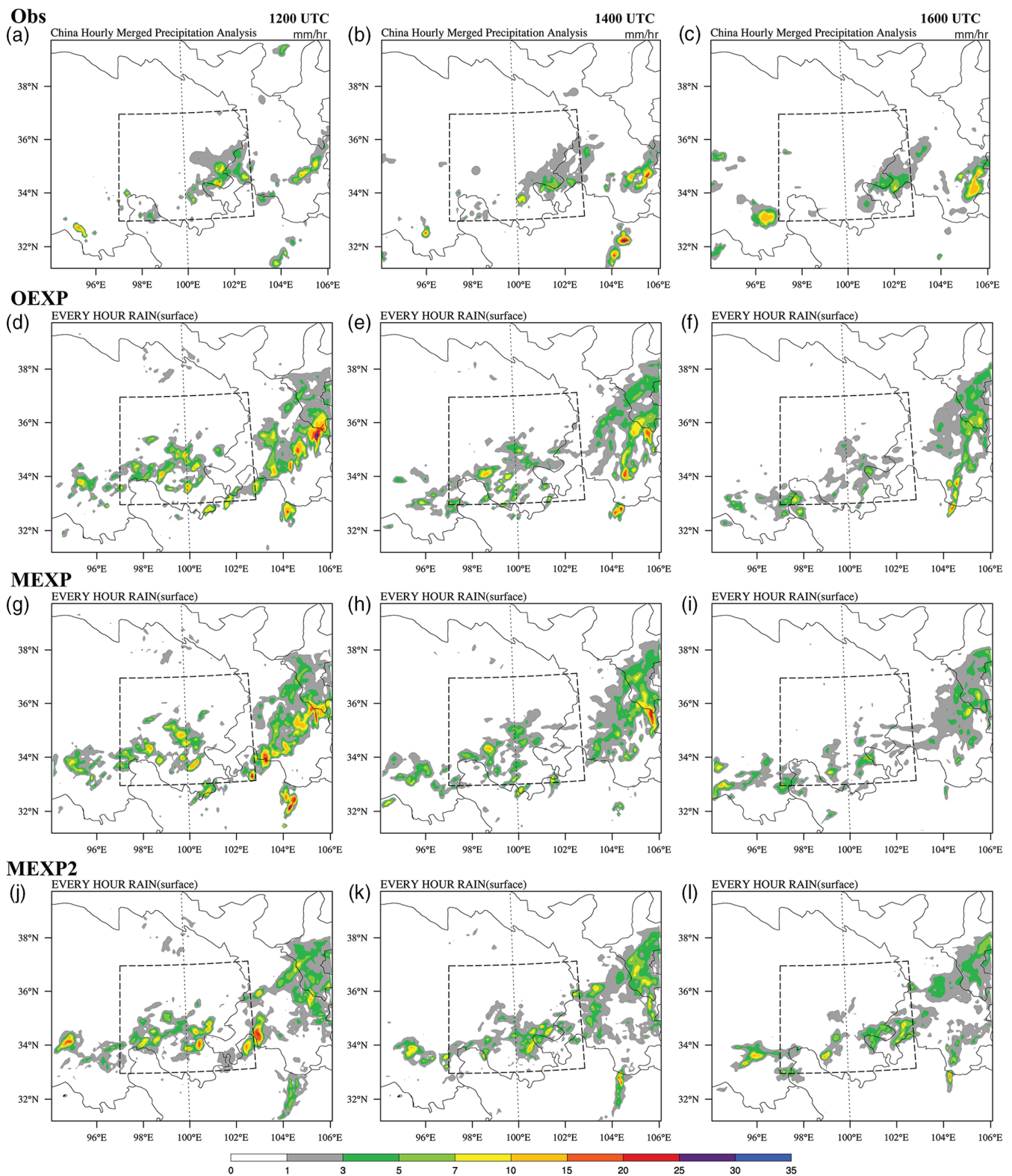


FIGURE 6 Same as Figure 5, but for Case 3 at 1200 UTC (left), 1400 UTC (middle) and 1600 UTC (right) on 17 August 2011

three experiments. Relating the rain intensities and positions of the Dulan and Xinghai stations to the observed 7 h accumulated rainfall area in Figure 2d, we find that Dulan Station occupied the fringes of the convective system, where the accumulated precipitation was below 10 mm. Xinghai Station was

much closer to the centre of the convective system, where the accumulated precipitation exceeded 35 mm. Thus, we located the edge and centre of the convective system at Dulan and Xinghai, respectively. Considering these locations, τ should be shorter at Dulan than at Xinghai. In OEXP-CU and

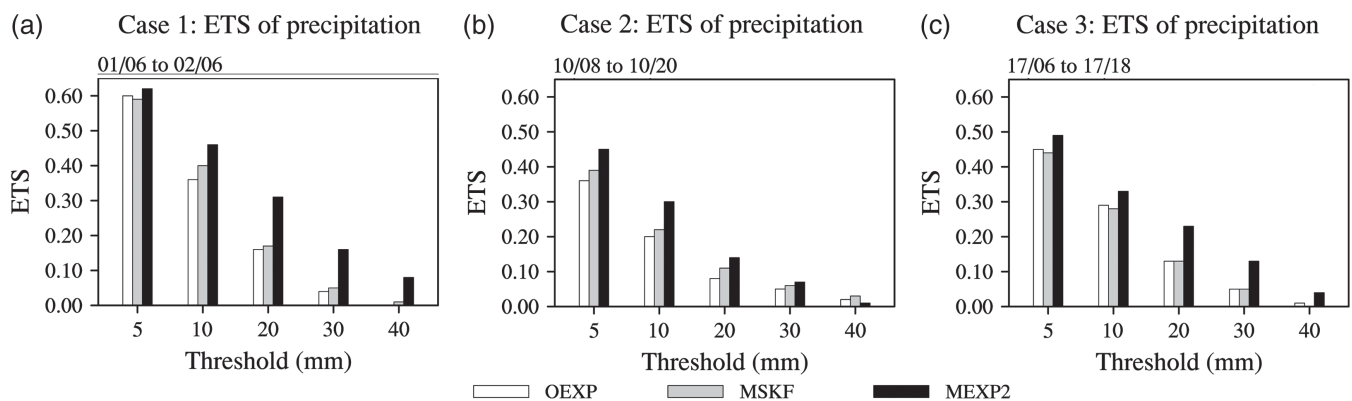


FIGURE 7 The ETS scores for (a) 24 h and (b,c) 12 h accumulated precipitation for (a) Case 1, (b) Case 2 and (c) Case 3 in different experiments against automatic station and CMORPH hourly precipitation fusion products with thresholds of 5, 10, 20, 30, 40 and 50 mm

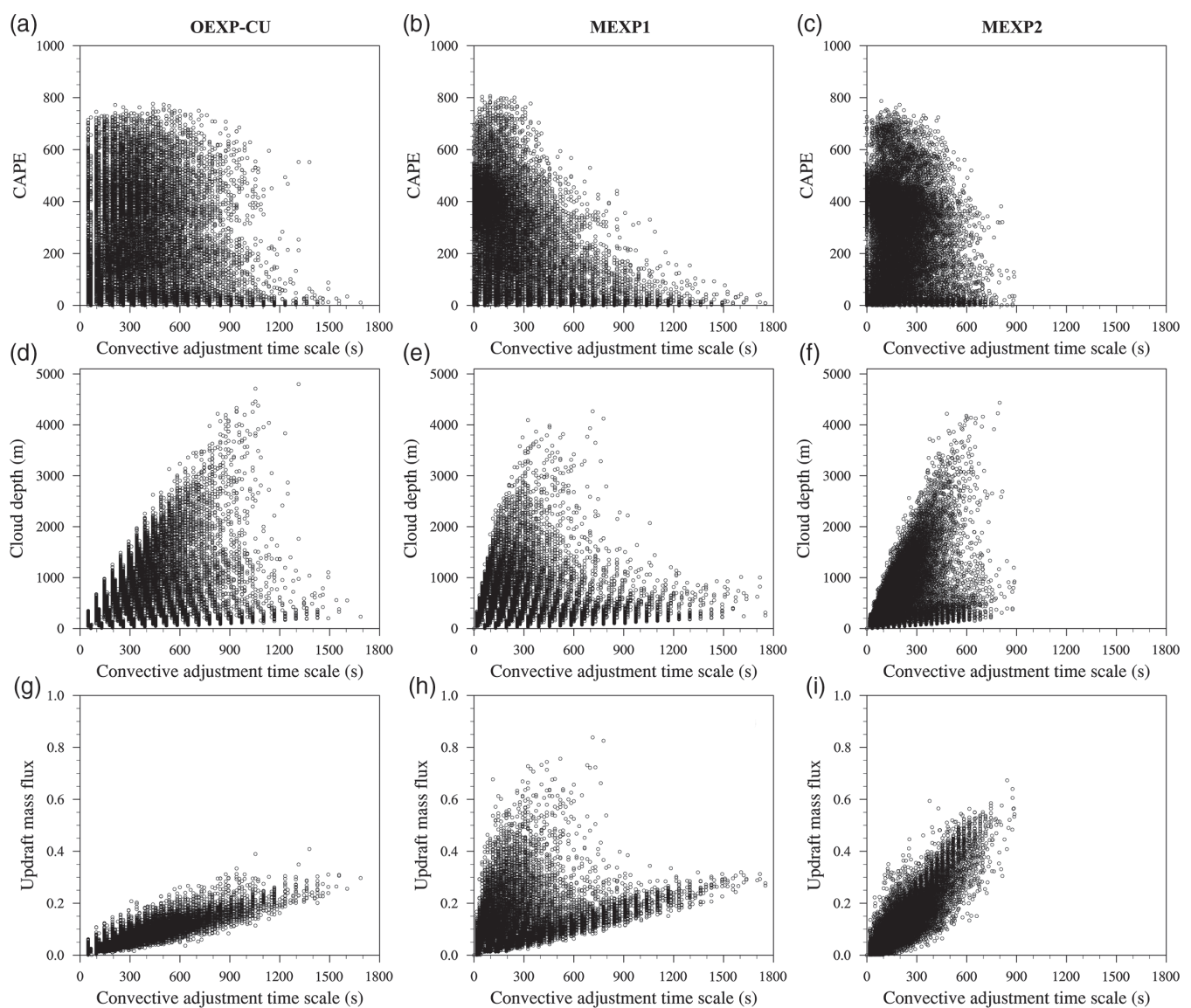


FIGURE 8 Scatterplots showing the time-averaged convective available potential energy (CAPE; J/kg) (top), cloud depth (m) (middle) and maximum Updraught Mass Flux (UMF) (bottom) of each grid column from the D03 outputs in Case 1, as functions of the time-averaged convective adjustment time-scale. Results were computed by OEXP-CU (left), MEXP1 (middle) and MEXP2 (right)

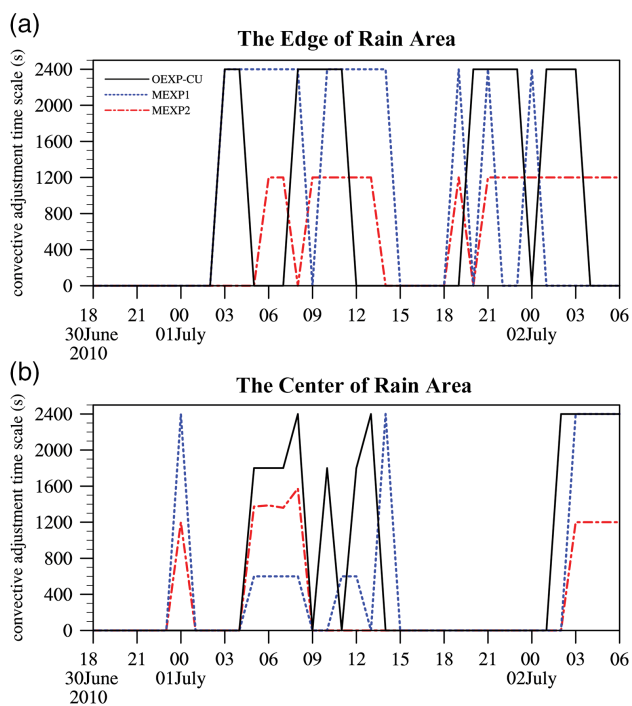


FIGURE 9 Time series of convective adjustment time-scale(s) from the D03 outputs in Case 1 at (a) Dulan Station and (b) Xinghai Station, computed by OEXP-CU (solid lines), MEXP1 (dotted lines), and MEXP2 (dash-dotted lines) [Colour figure can be viewed at wileyonlinelibrary.com].

MEXP1, τ was longer at Dulan than at Xinghai (Figure 9). In MEXP2, the τ values of Dulan were half those of OEXP-CU and MEXP1, and apparently reflect the real, rapid convective processes on subgrid scales (Figure 9a). The decreased τ implies a process in which the CPS acts to rapidly remove convective instability. At Xinghai, the convective adjustment time-scale remained longest in OEXP-CU ($\tau < 1,800$ s), was largely reduced in MEXP1 ($\tau < 600$ s) and was intermediate in MEXP2 (Figure 9b). These characteristics indicate that

the original method overestimates τ at the edge of the rain area (Figure 9a) and calculates a τ that is almost below the lower threshold (1,800 s in OEXP-CU and 600 s in MEXP1; Figure 9b) in the central rain area. As the convection in the central rain area is almost resolved by the grid cells, a higher τ implies that the microphysical processes are largely resolved in that region. Moreover, the high frequency of convective processes in MEXP2 (Figure 9b) further indicates that τ calculated by the original method cannot realistically capture the convective adjustment over the TP, in either OEXP-CU or MEXP1. This failure is especially apparent in high-resolution simulations, although MEXP1 (in which the threshold changes) outperforms OEXP-CU.

To elucidate the mechanism of the convective process, we plot the vertical UMF profiles from the D03 output at the Dulan and Xinghai stations in Figure 10. At 1800 LST (1000 UTC), a relatively scattered (shallow) convective cloud with a short τ passed over Dulan. At this time, the UMF profile was larger in MEXP2 (between 600 and 700 hPa) than in OEXP-CU and MEXP1, whose profiles are very similar (Figure 10a). At 1600 LST (0800 UTC), Xinghai was covered by a convective cloud with a deep and thick UMF (Figure 10b). Consistent with the observation, the UMF generated by MEXP2 remarkably increased and thickened at the Xinghai location, unlike in OEXP-CU. Therefore, MEXP2 captured the concentrated and stronger rainfall at this location, whereas MEXP1 yielded an overly strong UMF with deeper cloud depth and OEXP-CU exhibited a thinner UMF with a shallower cloud depth. This contrast highlights the poor performance of MEXP1, and the failure of OEXP-CU (thin cloud base and excessively shallow convective cloud depth in this model) to produce a vertical cloud structure consistent with observations.

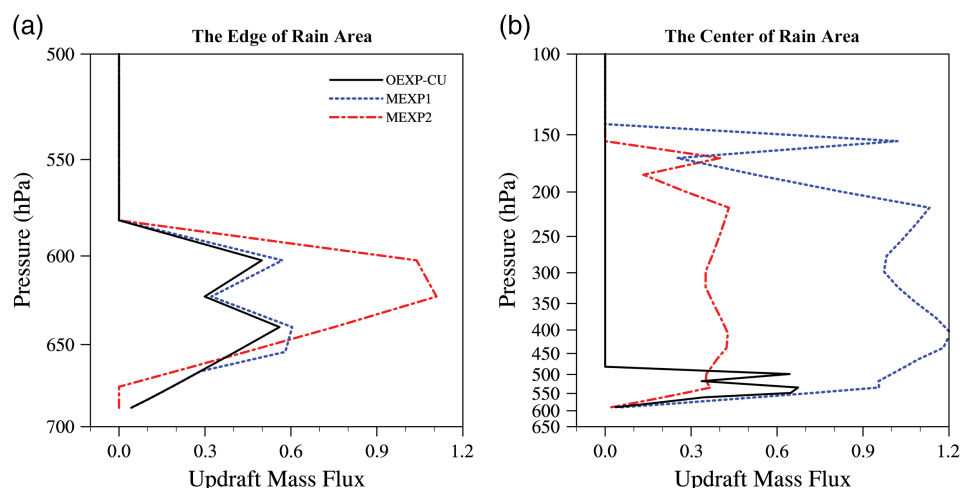


FIGURE 10 Vertical profile of updraught mass flux (UMF) in Case 1 on 1 July 2010, obtained from the D03 outputs at (a) Dulan Station at 1000 UTC and (b) Xinghai Station at 0800 UTC. Results were computed by OEXP-CU (solid lines), MEXP1 (dotted lines) and MEXP2 (dash-dotted lines) [Colour figure can be viewed at wileyonlinelibrary.com].

6 | SUMMARY AND CONCLUSION

This work proposes a new scheme of convective adjustment time-scale in the KFeta CPS and preliminarily validates its performance on three cases of convective precipitation events over the TP region. The BW scheme in this study is a good supplementary for the original KFeta scheme, which is more applicable in the grey zone than the multi-scale KF scheme and improves the simulated characteristics of convective cloud and its associated precipitation over the TP region in summer. In particular, it considers more detail regarding the process of vertical transport, the local and large-scale vertical movement reported by Zhang and McFarlane (1995), Bechtold *et al.* (2008) and Bullock *et al.* (2015), and the adjustment time of the convection. The small convective adjustment time-scale calculated in the BW scheme captures the parametrized convective process, increases the UMF and rapidly removes the instability at subgrid scales. Overall, the BW scheme more realistically modelled the convective characteristics than the original scheme in three cases and also proved applicable to high-resolution simulations without a scale-aware function for the TP area.

Scale-awareness provides a new perspective and approach for implementing the CPS in the grey zone, which should be acknowledged, applied, and optimized. The proposed modified scheme in this study should be a supplement for the scale-awareness in special cases and regions.

The experiments without considering the KF_cloud and radiation interaction are also carried out, which show a similar simulation performance, suggesting that the KF_cloud and radiation interaction is not a key factor that influences the simulation results for the TP region. Additional experiments solely considering the effect of subgrid cloud radius have not been included at present. More effects related to the parametrization of cloud radius would be investigated in future work. Other factors that are closely related to cloud characteristics in CPS, such as the initial dataset, are also important and worthy of future discussion. Thus, there are significant opportunities for further developments in mesoscale numerical simulations. The results of this study focused on three cases of convective precipitation over the TP. Future work should also focus on more cases with a larger sample size. Meanwhile, the modification of convective adjustment time-scale formulation should be universal for simulating all forms of relatively weak deep convection in the grey zone around the globe. Investigation of this idea through analysis of longer-term simulations will be the focus of our future work.

ACKNOWLEDGEMENTS

We would like to acknowledge the National Centers for Environmental Prediction for Operational Global Analysis data and the National Satellite Meteorological Center for satellite

imagery data. This work was supported by the NSFC (Nos. 91837205, 41805032, 41661144017, 91437217) and the China Special Fund for Meteorological Research in the Public Interest (Major projects) (GYHY201506001-4). We thank the Meteorology Information Center of the Chinese Meteorology Administration for providing observation data. We would like to thank the anonymous reviewers for reading and providing valuable comments. The authors would like to thank Enago (www.enago.cn) for the English language review.

CONFLICT OF INTEREST

All authors have no conflict of interest related to this work to declare.

ORCID

Chenghai Wang  <https://orcid.org/0000-0002-7122-7160>

REFERENCES

- Alapaty, K., Herwehe, J.A., Otte, T.L., Nolte, C.G., Bullock, O.R., Molland, M.S., Kain, J.S. and Dudhia, J. (2012) Introducing subgrid-scale cloud feedbacks to radiation for regional meteorological and climate modeling. *Geophysical Research Letters*, 39(24), L24809. <https://doi.org/10.1029/2012GL054031>.
- Arakawa, A. (1969) Parameterization of cumulus convection. *Proc. of the WMO/IUGG Symposium of Numerical Weather Prediction, Tokyo, Japan*. Japan Meteorological Society, pp. 1–6.
- Arakawa, A. and Schubert, W.H. (1974) Interaction of a cumulus cloud ensemble with the large-scale environment, part I. *Journal of the Atmospheric Sciences*, 31, 674–701. [https://doi.org/10.1175/1520-0469\(1974\)031<0674:IOACCE>2.0.CO;2](https://doi.org/10.1175/1520-0469(1974)031<0674:IOACCE>2.0.CO;2).
- Ban, N., Schmidli, J. and Schär, C. (2015) Heavy precipitation in a changing climate: does short-term summer precipitation increase faster? *Geophysical Research Letters*, 42, 1165–1172. <https://doi.org/10.1002/2014GL062588>.
- Bechtold, P., Köhler, M., Jung, T., Doblas-Reyes, F., Leutbecher, M., Rodwell, M.J., Vitart, F. and Balsamo, G. (2008) Advances in simulating atmospheric variability with the ECMWF model: from synoptic to decadal time-scales. *Quarterly Journal of the Royal Meteorological Society*, 134, 1337–1351. <https://doi.org/10.1002/qj.289>.
- Betts, A.K. (1986) A new convective adjustment scheme. Part I: Observational and theoretical basis. *Quarterly Journal of the Royal Meteorological Society*, 112(473), 677–691. <https://doi.org/10.1002/qj.49711247307>.
- Betts, A.K. (1997) The parameterization of deep convection. In: *The Physics and Parameterization of Moist Atmospheric Convection*, Vol. 505, pp. 255–279, NATO ASI series. Dordrecht: Springer.
- Betts, A.K. and Miller, M.J. (1986) A new convective adjustment scheme. Part II: Single column model tests using GATE wave, BOMEX, ATEX and arctic air-mass data sets. *Quarterly Journal of the Royal Meteorological Society*, 112, 693–709. <https://doi.org/10.1002/qj.49711247308>.
- Bony, S., Dufresne, J.L., Treut, H.L., Morcrette, J.J. and Senior, C. (2004) On dynamic and thermodynamic components of cloud

- changes. *Climate Dynamics*, 22, 71–86. <https://doi.org/10.1007/s00382-003-0369-6>.
- Boos, W.R. and Kuang, Z. (2010) Dominant control of the South Asian monsoon by orographic insulation versus plateau heating. *Nature*, 463(7278), 218–222. <https://doi.org/10.1038/nature08707>.
- Bretherton, C.S. and Smolarkiewicz, P.K. (1989) Gravity waves, compensating subsidence and detrainment around cumulus clouds. *Journal of the Atmospheric Sciences*, 46, 740–759.
- Bullock, O.R., Jr., Alapaty, K., Herwehe, J.A. and Kain, J.S. (2015) A dynamically computed convective time scale for the Kain–Fritsch convective parameterization scheme. *Monthly Weather Review*, 143(6), 2105–2120. <https://doi.org/10.1175/MWR-D-14-00251.1>.
- Bullock, O.R. Jr., Alapaty, K., Herwehe, J., Mallard, M. S., Otte, T. L., Gilliam, R. C. and Nolte, C. G. (2014) An observation-based investigation of nudging in WRF for downscaling surface climate information to 12-km grid spacing. *Journal of Applied Meteorology and Climatology*, 53, 20–33. <https://doi.org/10.1175/JAMC-D-13-030.1>.
- Chen, J., Wu, X., Yin, Y., Huang, Q. and Xiao, H. (2017) Characteristics of cloud systems over the Tibetan Plateau and east China during boreal summer. *Journal of Climate*, 30, 3117–3137. <https://doi.org/10.1175/JCLI-D-16-0169.1>.
- Cohen, B.G. and Craig, G.C. (2004) The response time of a convective cloud ensemble to a change in forcing. *Quarterly Journal of the Royal Meteorological Society*, 130(598), 933–944.
- Cohen, C. (2002) A comparison of cumulus parameterizations in idealized sea-breeze simulations. *Monthly Weather Review*, 130, 2554–2571. [https://doi.org/10.1175/1520-0493\(2002\)130<2554:ACOCPI>2.0.CO;2](https://doi.org/10.1175/1520-0493(2002)130<2554:ACOCPI>2.0.CO;2).
- Collins, W.D., Rasch, P.J., Boville, B.A., Hack, J.J., McCaa, J.R., Williamson, D.L., Briegleb, B.P., Bitz, C.M., Lin, S.-J. and Zhang, M.H. (2006) The formulation and atmospheric simulation of the Community Atmosphere Model version 3 (CAM3). *Journal of Climate*, 19, 2144–2161. <https://doi.org/10.1175/JCLI3760.1>.
- Deng, A. and Stauffer, D.R. (2006) On improving 4-km mesoscale model simulations. *Journal of Applied Meteorology and Climatology*, 45, 361–381. <https://doi.org/10.1175/JAM2341.1>.
- Dipankar, A., Stevens, B., Heinze, R., Moseley, C., Zangl, G., Giorgetta, M. and Brdar, S. (2015) Large eddy simulation using the general circulation model ICON. *Journal of Advances in Modeling Earth Systems*, 7, 963–986. <https://doi.org/10.1002/2015MS000431>.
- Done, J.M., Craig, G.C., Gray, S.L., Clark, P.A. and Gray, M.E.B. (2006) Mesoscale simulations of organized convection: importance of convective equilibrium. *Quarterly Journal of the Royal Meteorological Society*, 132, 737–756. <https://doi.org/10.1256/qj.04.84>.
- Dong, W., Lin, Y., Wright, J.S., Ming, Y., Xie, Y., Wang, B., Luo, Y., Huang, W., Huang, J., Wang, L., Tian, L., Peng, Y. and Xu, F. (2016) Summer rainfall over the southwestern Tibetan Plateau controlled by deep convection over the Indian subcontinent. *Nature Communications*, 7(3), 10925. <https://doi.org/10.1038/ncomms10925>.
- Dudhia, J. (1989) Numerical study of convection observed during the Winter Monsoon Experiment using a mesoscale two-dimensional model. *Journal of the Atmospheric Sciences*, 46, 3077–3107. [https://doi.org/10.1175/1520-0469\(1989\)046<3077:NSOCOD>2.0.CO;2](https://doi.org/10.1175/1520-0469(1989)046<3077:NSOCOD>2.0.CO;2).
- Emanuel, K.A., Neelin, J.D. and Bretherton, C.S. (1994) On large-scale circulations in convecting atmospheres. *Quarterly Journal of the Royal Meteorological Society*, 120, 1111–1143. <https://doi.org/10.1002/qj.49712051902>.
- Fu, R., Hu, Y., Wright, J.S., Jiang, J.H., Dickinson, R.E., Chen, M., Filipiak, M., Read, W.G., Waters, J.W. and Wu, D.L. (2006a) Short circuit of water vapor and polluted air to the global stratosphere by convective transport over the Tibetan Plateau. *Proceedings of the National Academy of Sciences*, 103(15), 5664–5669.
- Fu, Y. and Liu, G. (2007) Possible misidentification of rain type by TRMM PR over Tibetan Plateau. *Journal of Applied Meteorology and Climatology*, 46(5), 667–672. <https://doi.org/10.1175/JAM2484.1>.
- Gao, Y., Xu, J. and Chen, D. (2015) Evaluation of WRF mesoscale climate simulations over the Tibetan Plateau during 1979–2011. *Journal of Climate*, 28, 2823–2841. <https://doi.org/10.1175/JCLI-D-14-00300.1>.
- Gerard, L. (2015) Bulk mass-flux perturbation formulation for a unified approach of deep convection at high resolution. *Monthly Weather Review*, 143, 4038–4063. <https://doi.org/10.1175/MWR-D-15-0030.1>.
- Ghan, S., Randall, D., Xu, K.M., Cederwall, R., Cripe, D., Hack, J., Iacobellis, S., Klein, S., Krueger, S., Lohmann, U., Pedretti, J., Robock, A., Rotstayn, L., Somerville, R., Stenchikov, G., Sud, Y., Walker, G., Xie, S., Yio, J. and Zhang, M. (2000) A comparison of single column model simulations of summertime midlatitude continental convection. *Journal of Geophysical Research*, 105(D2), 2091–2124. <https://doi.org/10.1029/1999JD900971>.
- Grabowski, W., Xu, X. and Moncrieff, M.W. (1996) Cloud-resolving modeling of tropical cloud systems during phase III of GATE. Part I: Two dimensional experiments. *Journal of the Atmospheric Sciences*, 53, 3684–3709.
- Hong, S.-Y., Noh, Y. and Dudhia, J. (2006) A new vertical diffusion package with an explicit treatment of entrainment processes. *Monthly Weather Review*, 134, 2318–2341. <https://doi.org/10.1175/MWR3199.1>.
- Houze, R.A., Jr., Wilton, D.C. and Smull, B.F. (2007) Monsoon convection in the Himalayan region as seen by the TRMM Precipitation Radar. *Quarterly Journal of the Royal Meteorological Society*, 133, 1389–1411. <https://doi.org/10.1002/qj.106>.
- Huang, H.L., Wang, C.C., Chen, T.J. and Carbone, R.E. (2010) The role of diurnal solenoidal circulation on propagating rainfall episodes near the eastern Tibetan Plateau. *Monthly Weather Review*, 138(7), 2975–2989. <https://doi.org/10.1175/2010MWR3225.1>.
- Jiménez, P.A., Dudhia, J., González-Rouco, J.F., Navarro, J., Montávez, J.P. and García-Bustamante, E. (2012) A revised scheme for the WRF surface layer formulation. *Monthly Weather Review*, 140, 898–918.
- Kain, J.S. (2004) The Kain–Fritsch convective parameterization: an update. *Journal of Applied Meteorology*, 43, 170–181. [https://doi.org/10.1175/1520-0450\(2004\)043<0170:TKCPAU>2.0.CO;2](https://doi.org/10.1175/1520-0450(2004)043<0170:TKCPAU>2.0.CO;2).
- Kain, J.S., Baldwin, M.E. and Weiss, S.J. (2003) Parameterized updraft mass flux as a predictor of convective intensity. *Weather and Forecasting*, 18(1), 106–116. [https://doi.org/10.1175/1520-0434\(2003\)018<0106:PUMFAA>2.0.CO;2](https://doi.org/10.1175/1520-0434(2003)018<0106:PUMFAA>2.0.CO;2).
- Kain, J.S. and Fritsch, J.M. (1990) A one-dimensional entraining/detraining plume model and its application in convective parameterization. *Journal of the Atmospheric Sciences*, 47, 2784–2802. [https://doi.org/10.1175/1520-0469\(1990\)047<2784:AODEPM>2.0.CO;2](https://doi.org/10.1175/1520-0469(1990)047<2784:AODEPM>2.0.CO;2).
- Kain, J.S. and Fritsch, J.M. (1993) Convective parameterization for mesoscale models: the Kain–Fritsch scheme. In: *The Representation of Cumulus Convection in Numerical Models*, Meteor. Monogr., no. 24. Boston, MA: American Meteorological Society, pp. 165–170.
- Kain, J.S. and Fritsch, J.M. (1998) Multiscale convective overturning in mesoscale convective systems: reconciling observations, simulations, and theory. *Monthly Weather Review*, 126, 2254–2273. [https://doi.org/10.1175/1520-0493\(1998\)126<2254:MCOIMC>2.0.CO;2](https://doi.org/10.1175/1520-0493(1998)126<2254:MCOIMC>2.0.CO;2).

- Kalnay, E., Kanamitsu, M., Kistler, R., Collins, W., Deaven, D., Gandin, L., Iredell, M., Saha, S., White, G., Woollen, J., Zhu, Y., Chelliah, M., Ebisuzaki, W., Higgins, W., Janowiak, J., Mo, K.C., Ropelewski, C., Wang, J., Leetmaa, A., Reynolds, R., Jenne, R. and Joseph, D. (1996) The NCEP/NCAR 40-year reanalysis project. *Bulletin of the American Meteorological Society*, 77, 437–472. [https://doi.org/10.1175/1520-0477\(1996\)077<0437:TNYRP>2.0.CO;2](https://doi.org/10.1175/1520-0477(1996)077<0437:TNYRP>2.0.CO;2).
- Kuo, Y.H., Bresch, J.F., Cheng, M.D., Kain, J., Parsons, D.B., Tao, W.K. and Zhang, D.L. (1997) Summary of a mini workshop on cumulus parameterization for mesoscale models. *Bulletin of the American Meteorological Society*, 78(3), 475–491.
- Lean, H.W., Clark, P.A., Dixon, M., Roberts, N.M., Fitch, A., Forbes, R. and Halliwell, C. (2008) Characteristics of high-resolution versions of the Met Office Unified Model for forecasting convection over the United Kingdom. *Monthly Weather Review*, 136, 3408–3424. <https://doi.org/10.1175/2008MWR2332.1>.
- Li, Y. and Zhang, M. (2016) Cumulus over the Tibetan Plateau in the summer based on CloudSat-CALIPSO data. *Journal of Climate*, 29, 1219–1230. <https://doi.org/10.1175/JCLI-D-15-0492.1>.
- Lim, K.-S.S. and Hong, S.-Y. (2010) Development of an effective double-moment cloud microphysics scheme with prognostic cloud condensation nuclei (CCN) for weather and climate models. *Monthly Weather Review*, 138, 1587–1612. <https://doi.org/10.1175/2009MWR2968.1>.
- Luo, Y., Zhang, R., Qian, W., Luo, Z. and Hu, X. (2011) Intercomparison of deep convection over the Tibetan Plateau–Asian monsoon region and subtropical North America in boreal summer using CloudSat-CALIPSO data. *Journal of Climate*, 24(8), 2164–2177. <https://doi.org/10.1175/2010JCLI4032.1>.
- Mahoney, K.M. (2016) The representation of cumulus convection in high-resolution simulations of the 2013 Colorado Front Range flood. *Monthly Weather Review*, 144, 4265–4278. <https://doi.org/10.1175/MWR-D-16-0211.1>.
- Manabe, S., Smagorinsky, J. and Strickler, R.F. (1965) Simulated climatology of a general circulation model with a hydrological cycle. *Monthly Weather Review*, 93, 769–798. [https://doi.org/10.1175/1520-0493\(1965\)093,0769:SCOAGC.2.3.CO;2](https://doi.org/10.1175/1520-0493(1965)093,0769:SCOAGC.2.3.CO;2).
- Maussion, F., Scherer, D., Finkelburg, R., Richters, J., Yang, W. and Yao, T. (2011) WRF simulation of a precipitation event over the Tibetan Plateau, China – an assessment using remote sensing and ground observations. *Hydrology and Earth System Sciences*, 15(6), 1795–1817. <https://doi.org/10.5194/hess-15-1795-2011>.
- Mishra, S.K. and Srinivasan, J. (2010) Sensitivity of the simulated precipitation to changes in convective relaxation time scale. *Annals of Geophysics*, 28, 1827–1846. <https://doi.org/10.5194/angeo-28-1827-2010>.
- Miura, H. (2007) An upwind-biased conservative advection scheme for spherical hexagonal–pentagonal grids. *Monthly Weather Review*, 135, 4038–4044. <https://doi.org/10.1175/2007MWR2101.1>.
- Mlawer, E.J., Taubman, S.J., Brown, P.D., Iacono, M.J. and Clough, S.A. (1997) Radiative transfer for inhomogeneous atmospheres: RRTM, a validated correlated-k model for the longwave. *Journal of Geophysical Research*, 102, 16663–16682. <https://doi.org/10.1029/97JD00237>.
- Narita, M. (2010) Modification to the mixing rate of convective cloud in the Kain–Fritsch scheme. *CAS/JSC WGNE Research Activities in Atmospheric and Oceanic Modelling*, 40(Section 04), 11–12.
- Randall, D., Xu, K.M., Sommerville, R.J.C. and Iacobellis, S. (1996) Single-column models and cloud ensemble models as links between observations and climate models. *Journal of Climate*, 9, 1683–1697. [https://doi.org/10.1175/1520-0442\(1996\)009<1683:SCMACE>2.0.CO;2](https://doi.org/10.1175/1520-0442(1996)009<1683:SCMACE>2.0.CO;2).
- Romatschke, U., Medina, S. and Houze, R.A.J. (2010) Regional, seasonal, and diurnal variations of extreme convection in the South Asian region. *Journal of Climate*, 23, 419–439. <https://doi.org/10.1175/2009JCLI3140.1>.
- Satoh, M., Tomita, H., Yashiro, H., Miura, H., Kodama, C., Seiki, T., Noda, A.T., Yamada, Y., Goto, D., Sawada, M., Miyoshi, T., Niwa, Y., Hara, M., Ohno, T., Iga, S.I., Arakawa, T., Inoue, T. and Kubokawa, H. (2014) The non-hydrostatic icosahedral atmospheric model: description and development. *Progress in Earth and Planetary Sciences*, 1, 18. <https://doi.org/10.1186/s40645-014-0018-1>.
- Schlemmer, L., Hohenegger, C., Schmidli, J., Bretherton, C. S. and Schär, C. (2011) An idealized cloud-resolving framework for the study of midlatitude diurnal convection over land. *Journal of the Atmospheric Sciences*, 68, 1041–1057. <https://doi.org/10.1175/2010JAS3640.1>.
- Skamarock, W.C., Klemp, J.B., Dudhia, J., Gill, D.O., Barker, D.M., Wang, W. and Powers, J.G. (2008) *A description of the Advanced Research WRF version 3*. NCAR Tech. Note TN-475+STR, 113 pp.
- Stensrud, D.J. (2007) *Parameterization Schemes: Keys to Understanding Numerical Weather Prediction Models* (p.488). Cambridge: Cambridge University Press.
- Stevens, B. and Bony, S. (2013) What are climate models missing? *Science*, 340(6136), 1053–1054. <https://doi.org/10.1126/science.1237554>.
- Su, F., Duan, X., Chen, D., Hao, Z. and Cuo, L. (2013) Evaluation of the global climate models in the CMIP5 over the Tibetan Plateau. *Journal of Climate*, 26, 3187–3208. <https://doi.org/10.1175/JCLI-D-12-00321.1>.
- Tewari, M., Chen, F., Wang, W., Dudhia, J., Lemone, M. A., Mitchell, K., Ek, M., Gayno, G., Wegiel, J. and Cuenca, R.H. (2004) Implementation and verification of the unified Noah land surface model in the WRF model. In: *20th Conference on Weather Analysis and Forecasting/16th Conference on Numerical Weather Prediction*, pp. 11–15.
- Wang, C. and Yu, L. (2011) Sensitivity of regional climate model to different cumulus parameterization schemes in simulation of the Tibetan Plateau climate [in Chinese]. *Chinese Journal of Atmospheric Sciences*, 35(6), 1132–1144. <https://doi.org/10.3878/j.issn.1006-9895.2011.06.12>.
- Wang, K., Zhang, F., Sun, C. and Wang, C. (2014) Development and validation of WRF-WSM3 scheme in simulation of snowstorm in the Tibetan Plateau [in Chinese]. *Chinese Journal of Atmospheric Sciences*, 38(1), 101–109. <https://doi.org/10.3878/j.issn.1006-9895.2013.12170>.
- Wang, Y. and Wang, C. (2016) Features of clouds and convection during the pre- and post-onset periods of the Asian summer monsoon. *Theoretical and Applied Climatology*, 123(3), 551–564. <https://doi.org/10.1007/s00704-015-1372-7>.
- Weisman, M.L., Skamarock, W.C. and Klemp, J.B. (1997) The resolution dependence of explicitly modeled convective systems. *Monthly Weather Review*, 125, 527–548. [https://doi.org/10.1175/1520-0493\(1997\)125<0527:TRDOEM>2.0.CO;2](https://doi.org/10.1175/1520-0493(1997)125<0527:TRDOEM>2.0.CO;2).
- Wilks, D.S. (1995) *Statistical Methods in Atmospheric Sciences: An Introduction*. (Vol. 59, p.464) London: Academic Press.
- Xu, J., Zhang, B., Wang, M. and Wang, H. (2012) Diurnal variation of summer precipitation over the Tibetan Plateau: a cloud-resolving simulation. *Annals of Geophysics*, 30, 1575–1586. <https://doi.org/10.5194/angeo-30-1575-2012>.

- Xu, K., Arakawa, A. and Krueger, S.K. (1992) The macroscopic behavior of cumulus ensembles simulated by a cumulus ensemble model. *Journal of the Atmospheric Sciences*, 49, 2402–2420. [https://doi.org/10.1175/1520-0469\(1992\)049<2402:TMBOCE>2.0.CO;2](https://doi.org/10.1175/1520-0469(1992)049<2402:TMBOCE>2.0.CO;2).
- Xu, K.M. and Arakawa, A. (1992) Semi-prognostic tests of the Arakawa–Schubert cumulus parameterization using simulated data. *Journal of the Atmospheric Sciences*, 49, 2421–2436. [https://doi.org/10.1175/1520-0469\(1992\)049<2421:STOTAS>2.0.CO;2](https://doi.org/10.1175/1520-0469(1992)049<2421:STOTAS>2.0.CO;2).
- Xu, X., Lu, C., Shi, X. and Gao, S. (2008) World water tower: an atmospheric perspective. *Geophysical Research Letters*, 35(20), 525–530. <https://doi.org/10.1029/2008GL035867>.
- Yan, Y., Liu, Y. and Lu, J. (2016) Cloud vertical structure, precipitation, and cloud radiative effects over Tibetan Plateau and its neighboring regions: cloud and CRE over Tibetan Plateau. *Journal of Geophysical Research: Atmospheres*, 121(10), 5864–5877. <https://doi.org/10.1002/2015JD024591>.
- Zhang, C., Wang, Y. and Hamilton, K. (2011) Improved representation of boundary layer clouds over the southeast Pacific in ARW-WRF using a modified Tiedtke cumulus parameterization scheme. *Monthly Weather Review*, 139, 3489–3513. <https://doi.org/10.1175/MWR-D-10-05091.1>.
- Zhang, D.L., Hsie, E.Y. and Moncrieff, M.W. (1988) A comparison of explicit and implicit predictions of convective and stratiform precipitating weather systems with a meso- β -scale numerical model. *Quarterly Journal of the Royal Meteorological Society*, 114(479), 31–60. <https://doi.org/10.1002/qj.49711447903>.
- Zhang, G.J. and McFarlane, N.A. (1995) Sensitivity of climate simulations to the parameterization of cumulus convection in the Canadian climate centre general circulation model. *Atmosphere–Ocean*, 33(3), 407–446. <https://doi.org/10.1080/07055900.1995.9649539>.
- Zheng, Y., Alapaty, K., Herwehe, J.A., del Genio, A.D. and Niyogi, D. (2016) Improving high-resolution weather forecasts using the Weather Research and Forecasting (WRF) model with an updated Kain–Fritsch scheme. *Monthly Weather Review*, 144, 833–860. <https://doi.org/10.1175/MWR-D-15-0005.1>.

How to cite this article: Wang C, Wu D, Zhang F. Modification of the convective adjustment time-scale in the Kain–Fritsch eta scheme for the case of weakly forced deep convection over the Tibetan Plateau region. *Q J R Meteorol Soc*. 2019;145:1915–1932. <https://doi.org/10.1002/qj.3535>